Geomechanics and Engineering, *Vol. 29, No. 3 (2022) 339-348*
https://doi.org/10.12989/gae.2022.29.3.339

Measures to control deformation in deep excavation for cut and cover tunneling

Kyu-Tae Nam[1], Jae-Ho Jeong[2], Seung-Hyun Kim[3], Kang-Hyun Kim[3] and Jong-Ho Shin*[3]

[1]*Dohwa Engineering, 438 Samseong-ro, Gangnam-gu, Seoul 06178, Korea*
[2]*SYTEC, Seoul, 145 Anam-ro, Seongbuk-gu, Seoul 02841, Korea*
[3]*Department of Civil Engineering, Konkuk University, Seoul 05029, Korea*

(Received December 12, 2021, Revised February 24, 2022, Accepted March 2, 2022)

Abstract. The bored tunneling method is generally preferred for urban tunnel construction, However the cut & cover tunnel is still necessary for special conditions, such as metro station and access structures. In some case, deep excavation for cut & cover construction is planed of irregular and unusual shape, as a consequence, the convex and concave corner is often encountered during that excavation. In particular, discontinuity or imbalance of the support structure in the convex corner can lead to collapse, which may result in damages and casualties. In this study, the behavior of the convex corner of retaining structure were investigated using 3-dimensional numerical models established to be able to simulate the split-shaped behavior of convex corners. To improve the stability in the vicinity of the convex corner, several stabilizing measures were proposed and estimated numerically. It is found that linking two discretized wales at the convex corner can effectively perform the control of deformation. Furthermore, it was also confirmed that the stabilizing measures can be enhanced when the tie-material linking two discretized wales is installed at the depth of the maximum wall deflection.

Keywords: convex corner; deep excavation; ground surface settlement; split-shaped behavior; wall deformation mode

1. Introduction

Bored tunneling has been increasingly chosen in preference as the construction method to avoid negative social impact urban underground development projects. However, in such cases, deep excavation for cut & cover tunnel in partial section has been inevitable for special conditions, such as metro station and access structures.

The layout of excavation is generally planned as rectangular shape, however, due to the complexity and restrictions of urban geometry, the excavation sometimes is irregular and unusual shape (Zheng *et al.* 2017). As a consequence, the convex and concave corners are often encountered in the excavation process as shown in Fig. 1.

Mechanical behavior at the corner of excavation is obviously distinguished from those in middle positions of excavation. However, most previous studies on 3-dimensional effect at the corner of excavation have foused on the concave corners of rectangular shape (Ou *et al*. 1996, Lee *et al*. 1998, Finno and Roboski 2005, Zdravkovic *et al*. 2005, Finno *et al*. 2007, Lee and Kim 2008, Tan *et al.* 2013). They showed that a concave corner excavation is less disadvantageous in terms of stability of wall deformation and ground settlement behind the wall as compared to the middle position of excavation due to the 3-dimensional constraint effect. As a consequence, 2-dimensional model is mainly used in practice for stability analysis of deep excavation to achieve conservative construction principle and cost saving by minimizing time-consuming process. 2-dimension analysis generally uses FEM method (Mabsouri and Ebrahim 2019, Qian *et al.* 2019, Xiang *et al.* 2018, Zhang *et al.* 2018).

Several studies of recent years have pointed out that the convex corner yields a dangerous stress state with stress concentration, contrary to the concave corner which has beneficial effect of 3-dimensional constraint behavior. The concentrated unloading effect on the convex corner from two excavated sides strongly affects the soil mechanical behavior, and even causes a wedge-shaped failure surface around the corner area (Wei *et al*. 2009, Nian *et al*. 2012, Zhang *et al.* 2013a, Zhang *et al*. 2013b). Related to this behavior, a number of collapsed instances have been reported at various excavation sites and one of them in shown in Fig. 2.

Most of investigations for those instances resulted that the support of earth retaining structure did not sufficiently carry its design capacity due to the 'slip of the wale' at the convex corner which arose subsequent to concentrated deformation as mentioned above.

Although, several studies reported that the convex corner in the retaining structure can cause greater deformation than other excavation boundaries (Zhang *et al*. 2011, Zhao *et al.* 2015, Szepeshazi *et al*. 2016, Imeni *et al*. 2017), there is still a lack of research that investigates mechanical measures for enhancing stability of the retaining structure at the convex corner where the support is discretized structurally.

In this study, the 3-dimensional numerical analysis performed to propose measures of reinforcement to enhance the structural stability of the convex corner.

*Corresponding author, Professor
E-mail: jhshin@konkuk.ac.kr

Copyright © 2022 Techno-Press, Ltd.

ISSN: 2005-307X (Print), 2092-6219 (Online)

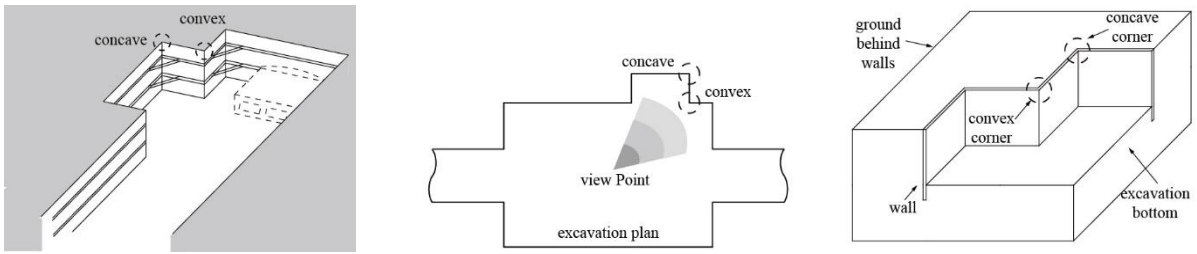

Fig. 1 Convex and concave corner of Deep cut & cover tunnel

Fig. 2 Collapse of convex corner in deep excavation

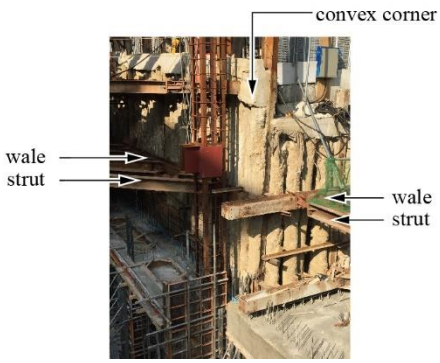

Fig. 3 Support elements of retaining structure at the convex corner

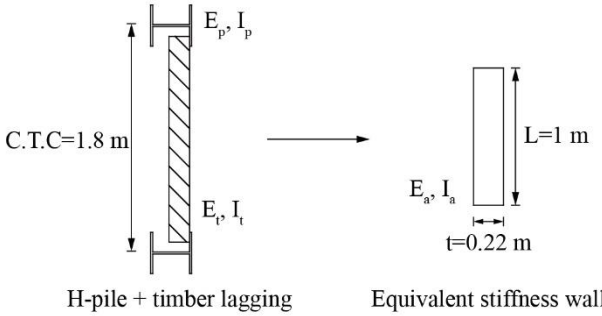

Fig. 4 Transposition concept of equivalent stiffness

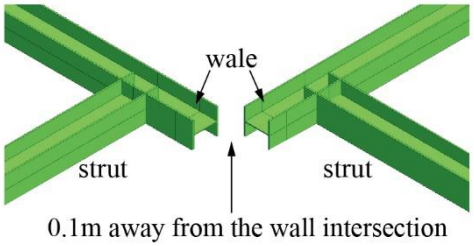

Fig. 5 Modeling of the discretized feature for the support members at convex corner

2. Numerical analysis modeling

2.1 Considerations for modeling

As the shape of the convex corner is different from that of the middle section, there must be a discretization of the support member at the intersection of two excavated sides as shown in Fig. 3. Furthermore, in spite of complex condition for construction, setting up a more strengthened support structure for convex corner is required considering concentration of stress and deformation due to the convex effect.

Several numerical techniques were specifically considered for modeling to simulate the convex corner effect as follows.

2.1.1 Modeling of retaining wall and supported structure

The retaining wall composed of H-shaped steel beam and wooden lagging was numerically modeled using an isotropic linear-elastic shell element. To represent the wall of composite materials using shell element, transposition concept of the equivalent stiffness was applied as shown in Fig. 4. The equivalent elastic modulus for the shell elements can be calculated using equation Eq. (1) (Jeong and Kim 2009).

$$E_p I_p \times N_p + E_t I_t \times N_t = E_a I_a \quad (1)$$

where, E_p is the elastic modulus of the H-Pile, I_p is the second moment of section of the H-Pile, N_p is the number of H-piles per unit width, E_t is the elastic modulus of the lagging, I_t is the second moment of the lagging, N_t is the number of lagging per unit width, E_a and I_a are the equivalent elastic modulus and the cross-sectional second moment of the wall respectively.

The numerical model for strut at the intersection of the convex corner using beam elements was built to simulate the discretized feature of support members at the convex corner correctly, which can cause split-shaped behavior of each wall at the intersection of two excavated sides (Fig. 5). This modeling method is beneficial, as it prevents the overestimation of support stiffness at the intersection of convex corner induced by superposition of node at each end of beam elements from two excavated sides.

2.1.2 Modeling consideration for ground-structure interaction

To simulate soil-structure slip behavior properly,

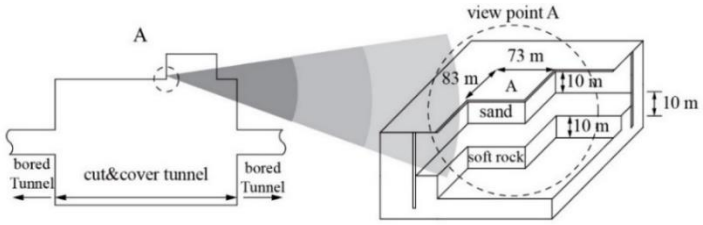

(a) Dimensions for 3D finite element model

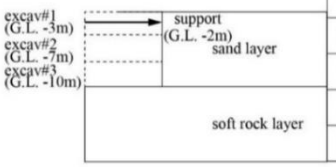

No.	Construction Stage	Contents
1	Initial state	calculation of initial stress
2	Wall installation	wall installation & displacament initialization
3	First excavation	excavation until G.L. -3m
4	Second excavation & supported installation	excavation & supported installation until G.L. -7m
5	Third excavation	excavation until G.L. -10m

(b) Construction stages for modeling excavation

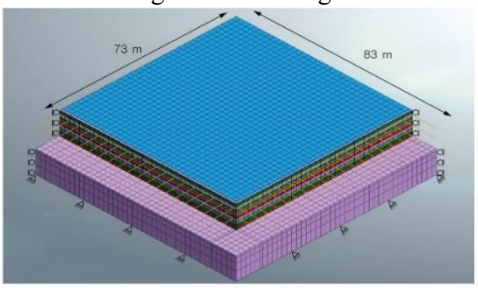

(c) Numerical model

Fig. 6 3D modeling of excavation of convex corner

interface elements of zero-thickness (Shin 2015) were used between the soil and shell elements of the wall. The characteristics of the interface elements are defined using Eqs. (2)-(5) (Yu *et al*. 2015).

$$K_n = E_{oed,i}/t_v \tag{2}$$

$$K_t = G_i/t_v \tag{3}$$

$$c_i = R \times /c_{soil} \tag{4}$$

$$tan\theta_i = R \times tan\theta_{soil} \tag{5}$$

where, $E_{oed,i} = 2 \times G_i \times \frac{(1-\mu_i)}{(1-2\mu_i)}$is the virtual thickness, $G_i = R^2 \times G_{soil}(G_{soil} = \frac{E}{2(1+\mu_{soil})})$; R is the strength reduction coefficient depending on the condition of the ground-structure interface. Empirical R value proposed by MIDAS (2013) is in the range of 0.6~0.7 for the soil-steel interface.

2.1.3 Modeling consideration for wall-wall interaction

Similar to the ground-structure interface, interface elements were also used to simulate the behavior between shell elements of the wall, which simulates split behavior of the wall at the intersection of two excavated sides.

2.2 3D Finite element model

Table 1 Application of excavation modeling elements for convex corner

Construction element	Ground	Wall	Wale	Strut
Element type	Solid(3D)	Shell(2D)	Beam(1D)	Beam(1D)

2.2.1 Geometry

The established 3D finite element model is as shown in Fig. 6. The dimensions of the excavation are 10 m in both depth and width, while those of the whole model is 20 m in depth and 83 m in width and length as shown in Fig. 6(a). The whole width and length on sides of the model was defined at least 7 times as long as the excavation depth referred to the distance (D), $D \geq 5\sim7\ H_e$(Finno *et al*. 2007) to make sure that the convex effect induced by excavation is sufficiently covered in the range of the established model.

The analysis sequences of soil excavation and support installation were carried out in 5 construction stages,

Considering 3 excavation steps. The numerical elements to simulate the excavation of the convex corner are detailed in Table 1.

The finite element mesh and boundary conditions are shown Fig. 6(c). Fixed displacement condition was applied to the direction of Z at the bottom and the side of the model. Whole nodes of the excavation boundaries are free to displace.

Table 2 Mechanical properties of geological strata

Ground	Model	E (kN/m^2)	v	γ (kN/m^3)	c (kN/m^2)	$\emptyset$ (°)	ψ(°)	K_0
Soil	MC	30,000	0.2	18	0	30	5	0.5
Soft rock	Elastic	200,000	0.3	18	-	-	-	-

Table 3 Structural properties of walls and supports

Structure	Model	E (kN/m^2)	v	A (m^2)	I (m^4)
Retaining wall	Elastic	28×106	0.2	0.22	8.87×10^{-4}
Strut/Wale	Elastic	20×107	0.2	0.012	2.04×10^{-4}

※ Cross section of strut/wale : H 300×300×10/15

Table 4 Wall-Ground interface element properties

K_n (kN/m^3)	K_t (kN/m^3)	R	$\emptyset_i$ (°)	c_i (kN/m^2)	ψ_i(°)
673,750	61,250	0.7	22	0	0

Table 5 Properties of interface elements between convex corner walls

K_n (kN/m^3)	K_t (kN/m^3)	R	$\emptyset_i$ (°)	c_i (kN/m^2)	ψ_i(°)
0	0	-	-	-	-

To justify the numerical model, preliminary analyses were carried out and the results were compared with those from other results (zhao *et al*. 2015). It is confirmed that the the numerical results were shown the same trends as the previous research (Yoo 2001).

2.2.2 Model parameters

Table 2 shows the mechanical properties of geological strata of the model. The soft rock layer that is supposed to show little deformation due to its high stiffness was represented as linear elastic material, and the soil layer was defined as a linear elastic-perfectly plastic model with Mohr-Coulomb failure criteria adopting the non-associated flow rule to minimize overestimation of the volumetric strain of the soil.

The retaining wall was represented using shell element as mentioned above, where strut and wale (H-shaped steel support member, H 300×300×10/15) were defined as linear-elastic beam elements. Table 3 shows the structural properties of the retaining structure.

Tables 4 and 5 shows the properties of interfaces that simulate the interaction of ground-structure and wall-wall. The properties of the interface between wall and wall are set considering minimization of the influence induced by stiffness of the interfaces.

3. Behavior of convex corner during excavation

3.1 Constrained conditions

The retaining wall at the intersection of the convex corner can be assumed to behave as a continuum member defined as attached (constrained) boundary condition as shown in Fig. 7(a).

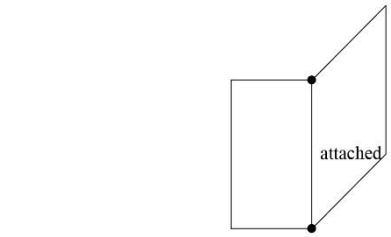

(a) Edge attached

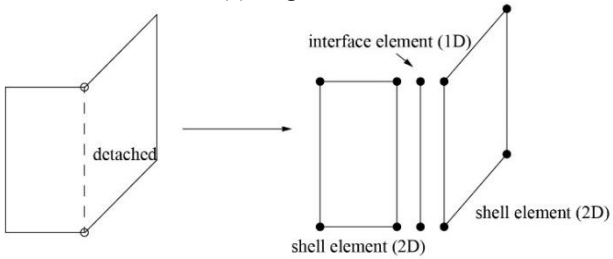

(b) Edge detached and Details

Fig. 7 Modeling method the wall at the convex corner

On the other hand, it can also be assumed that that two walls at the intersection from each excavation side behave independently as discontinued members defined as detached (non-constrained) boundary condition that may cause a split-shape of deformation between two walls as shown in Fig. 7(b). Numerical analysis was performed on the two model conditions mentioned above and the results are shown in Fig. 8.

From the result that ground surface settlement behind the wall and wall deflection is decreased in the case of attached condition compared to detached condition, it is confirmed that constrained support structure is valid for controlling split-up behavior of the intersection at the convex corner. Therefore, a proper reinforcing measure

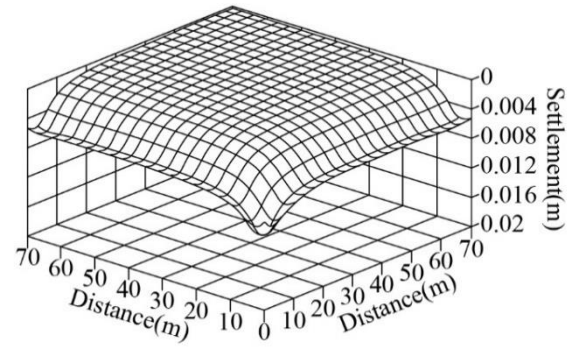

(a) Ground settlement in detached condition

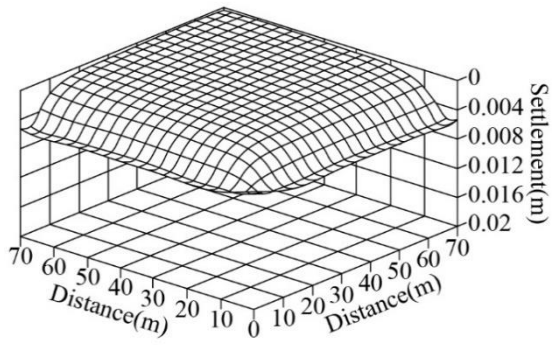

(b) Ground settlement in attached condition

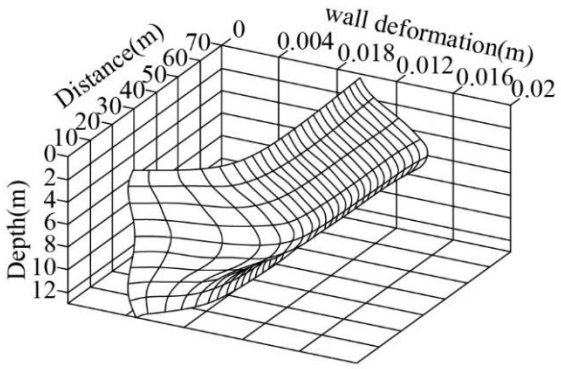

(c) Wall deflection for detached condition

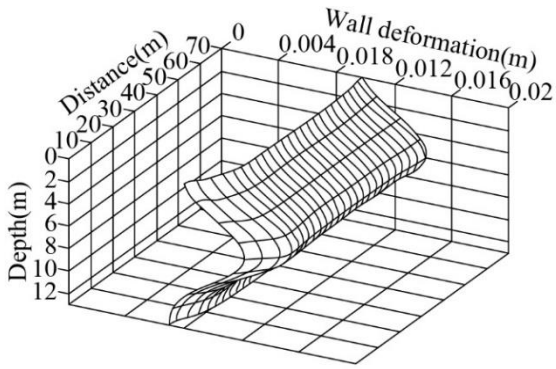

(d) Wall deflection for attached condition

Fig. 8 Results for constrained conditions of intersection at the convex corner

linking two walls of each excavated side to make it behave as a continuum structure can be effective modeling to control vulnerable behavior of convex corner.

Based on these results, the detached condition was chosen for the boundary condition of the numerical model to investigate the characteristics of behavior of the convex corner, which can be considered as a conservative manner.

3.2 Behavior of ground and retaining wall

(1) Settlement and deformation

Ground surface settlement behind the wall and wall deflection by the convex corner is analyzed so that the comprehensive trend of deformation and the affected range of convex corner can be discussed.

Fig. 9 shows the result of ground settlement behind the wall in the final excavation stage. As distance from the convex corner increases, the settlement at the corner and affected area of the corner decreases gradually until the settlement curve is converged to the same value of the plane strain condition at the distance of $1.1\,H_e$ (H_e , final excavation depth).

The maximum settlement is obtained at the distance of $0.3H_e$, and the value of maximum settlement in the convex corner was 2.2 times larger than the value of plane strain condition.

As shown in Fig. 10, the wall deflection is minimized in the vicinity of the convex corner increasing gradually until the distance reaches $0.7\,H_e$ and the trend of deflection maintains steady.

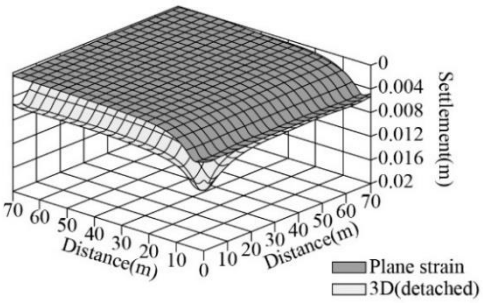

Fig. 9 Distribution of the ground surface settlement behind the wall

With regard to the result of plane strain condition, the wall deflection trend is similar to that of the 3D analysis at the range of distance over $0.7\,H_e$, but the maximum deflection is calculated to be 1.1 times larger than that of the 3D analysis. rom the above result, it can be stated that the affected range of the convex corner is within the distance of $0.7H_e$ from the corner.

(2) Bending moment of the wall

To investigate the characteristics of internal force in the wall at the convex corner, the bending moments resulting from the plane strain condition and 3D analysis are described in Fig. 11.

The 3-dimensional distribution of bending moment shows practically same value as that of plane strain condition, however, at the closest location from the convex corner, it is decreased to the value of almost zero that means very small value compared to that of plain strain condition.

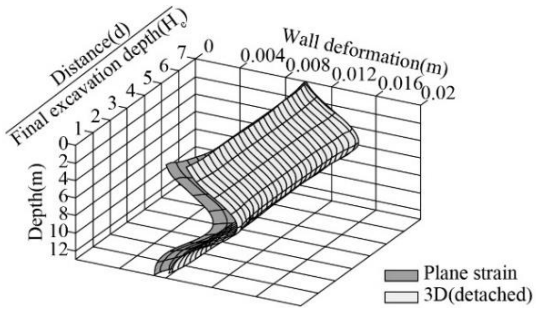

Fig. 10 Distribution of the wall deflection

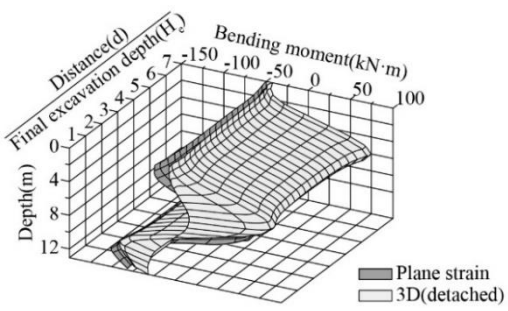

Fig. 11 Distribution of bending moment of the wall

As previously reported by Szepeshazi *et al*. (2016), it is reconfirmed that the maximum value of bending moment is calculated at the depth of $1/3H_e$ near the bottom of the excavation.

(3) Stress path of the ground

The stress path of the ground according to the construction stage was analyzed for the point (A) that is at the convex corner and the point (B) in the middle section that is not affected by the corner effect as shown in Fig. 12.

The generalized 3D stress behavior can be expressed in the way of considering the 3D stress parameters such as volumetric stress invariant (p') and shear stress invariant (J). 3D stress parameters can be calculated from Eq. (6) and Eq. (7).

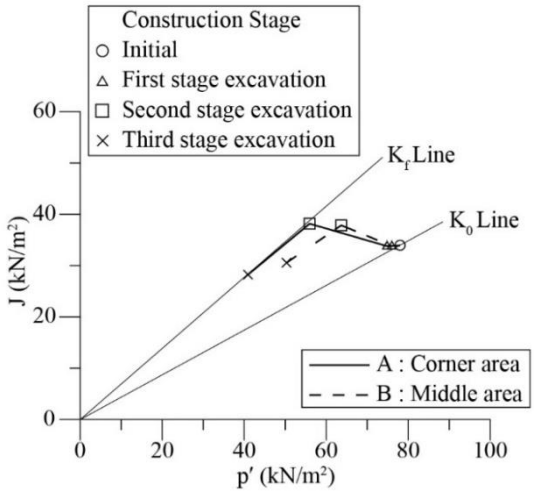

Fig. 12 Stress path in the process of excavation

Mohr-Coulomb failure criteria used in this study to simulate plastic behavior of the ground can be 3-dimensionally schematized introducing volumetric stress invariant (p') and shear stress invariant (J) in 2D $p'-J$ plane. Mohr-Coulomb failure criteria using 3D stress invariants of deviatoric stress plane is as belows

$$p' = \frac{\sigma_1+\sigma_2+\sigma_3}{3} \tag{6}$$

$$J = \frac{1}{\sqrt{6}}(\sqrt{(\sigma_1-\sigma_2)^2+(\sigma_2-\sigma_3)^2+(\sigma_3-\sigma_1)^2}) \tag{7}$$

Mohr-Coulomb failure criteria used in this study to simulate plastic behavior of the ground can be 3-dimensionally schematized introducing volumetric stress invariant (p') and shear stress invariant (J) in 2D $p'-J$ plane. Mohr-Coulomb failure criteria using 3D stress invariants of deviatoric stress plane is as belows

$$F(\sigma') = \frac{J}{(p'+a)g_f(\theta_L)} - 1 = 0 \tag{8}$$

where a is the $p'-J$ axis intercept (p') of the $a = c'/\tan\phi'$ coordinate system, in $\sigma_1 \geq \sigma_2 \geq \sigma_3$ and $-\pi/6 \geq \theta_L \geq \pi/6$.

$$g_f(\theta_L) = \frac{sin\,\emptyset'}{cos\,\theta_L + \frac{1}{\sqrt{3}}sin\,\theta_L\,sin\,\emptyset'} \tag{9}$$

$$\theta_L = tan^{-1}\left[\frac{(2b-1)}{\sqrt{3}}\right], \qquad b = \frac{\sigma_2'-\sigma_3'}{\sigma_1'-\sigma_3'} \tag{10}$$

Fig. 12 describes the stress path and failure line on the $p'-J$ plane using Eqs.(8)-(10).

The stress path of each point shows similar pattern during excavation stages, however, stress path of point A is varied in wider range than that of point B.

In respect of geotechnical stability, two points are in unfavorable state at 2nd construction stage and the stress path of point A is stretched to the failure line which implies that the ground area adjacent of the convex corner is failed and in plastic state.

4. Measures to control deformation at the convex corner

4.1 Cases of measures

The result of analysis for the behavior of convex effect shows unfavorable effect especially in the aspect of increasing surface settlement behind the wall. The unfavorable effect is induced by the split-shaped deformed wall of the convex corner within certain affected range. Therefore, two cases of specific measures to control the split-shaped deformation at the convex corner was introduced and analyzed numerically.

One of the measures is to link two discretized wale at the intersection of the convex corner using a tie-material so that control the deformation functioning as a continuum member, and the other is to link two points on the upper end

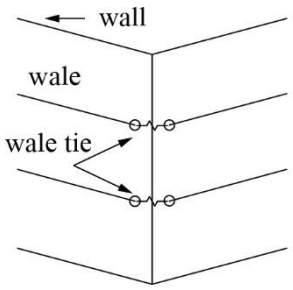

(a) Coupling the ends of the wale with a tie material

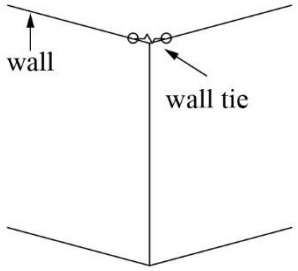

(b) Coupling the upper part of the wall with a tie material

Fig. 13 Cases of specific measures for the convex corner

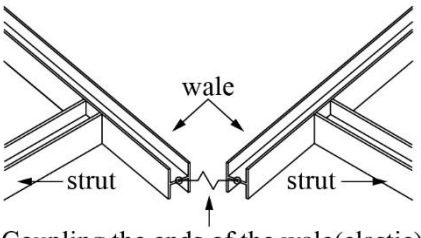

(a) Wale end coupling

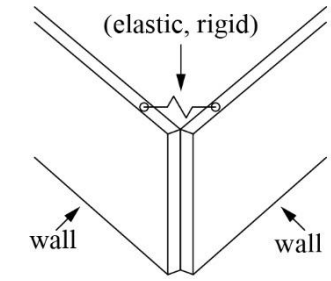

(b) Wall top coupling

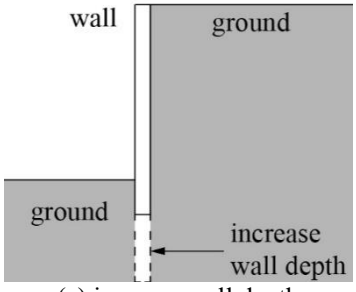

(c) increase wall depth

Fig. 14 Modeling of stabilizing measures

of each wall at two excavated sides with a tie-material as shown in Fig. 13.

Increasing embedded depth of the wall, one of the most commonly used stabilizing measures for retaining wall, was compared with the proposed specific reinforcing measures

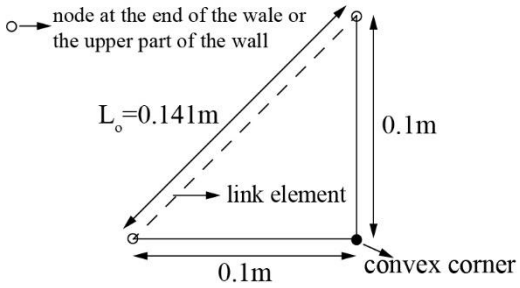

Fig. 15 Link element

Table 6 Analysis cases for each stabilizing measures

Measures	Details	Index
None	· Strut+Wale	General
Wale Link	· Strut+Wale+tie(Wale)	
	-install at 1st Wale (G.L. -2 m)	First Wale
	-install at 2nd Wale (G.L. -6 m)	Second Wale
	-install at both Wale (G.L. -2 m, -6 m)	Both Wale
Wall Link	·Strut+Wale+tie (Wall top)	
	- Elastic	Top Elastic
	- Rigid	Top Rigid
Increasing wall depth	· Strut+Wale	
	-Wall depth 0.6H$_e$ (H$_e$ = 10 m)	Depth 0.6H$_e$
	-Wall depth 0.9H$_e$	Depth 0.9H$_e$

to evaluate the validity. Fig.14 shows the modeling method of each measure

The tie-material that is defined based on a length of PC strand for earth anchors was numerically simulated using a link element as shown in Fig. 15. The link element was defined as a linear-elastic member that transfers tensile force only, and the spring constant (k) for mechanical stiffness is calculated using Eq. (11).

Details of analysis cases are shown in Table 6.

$$F = \left(\frac{EA}{L_0}\right)\Delta L = kx, \qquad k = 179{,}148(kN/m) \qquad (11)$$

where, $E = E_{steel} = 200\ GPa,\ A = A_{strand} = \frac{\pi}{4}(12.7 \times 10^{-3})^2\ m^2, L_0 = 0.141\ m, \Delta L = x$ (tensile strain of the material).

4.2 Results of analysis for each proposed measures

The numerical models for each measure were analyzed considering the result that was previously discussed in Section 3.

Ground surface settlement behind the wall and wall deflection were selected as key factors for interpretation of deformation behaviors, and lateral earth pressure and wall bending moment were selected to investigate mechanical behavior of the wall.

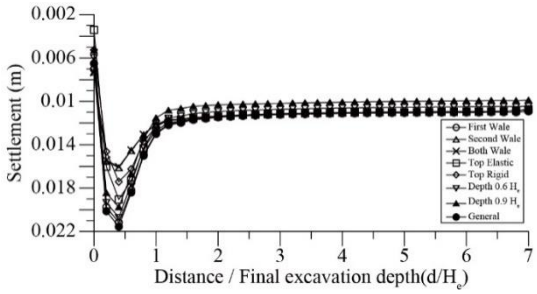

Fig. 16 Ground surface settlement behind the wall for each case of stabilizing measures

The interpretation was performed for the result of final excavation stage of analyses. The data extracted from the element at the distance of $0.3H_e$ where the maximum surface settlement had been observed was used for deformation analysis based on the result in Section 3.2. Deflection and bending moment of the wall extracted from the element of same location as in deformation analysis were used to investigate mechanical behavior of the wall.

(1) Ground behavior

Characteristics of deformation behavior of ground by proposed stabilizing measures is shown in Fig. 16. It can be stated that the maximum ground surface settlement behind the wall appears at the distance of $0.3H_e$ which is the same as discussed in Section 3.2 for the behavior of the convex corner without any measures.

On comparing the maximum settlement ratio of each measure, Cases indexed 'Second wale', 'Both wale' and 'Top rigid' shows more effective performance of controlling the ground surface settlement behind the wall than the others. Measures indexed 'Second wale' and 'Both wale' lowers settlement level to 74% of the case indexed 'General' which was numerically modeled without any specific measures. The maximum settlement of the case indexed 'Top rigid' reaches 81% of the case indexed 'General'.

(2) Wall deflection

Characteristics of deformation behavior by proposed stabilizing measures is described in Fig. 17. With regard to wall deflection in the cross-section at the distance of 0.3He, the maximum deflection is observed at the depth of G.L. -6m. while the deflection of the upper range is decreased because of the effect of strut installed at the depth of G.L. -2m in the 1st excavation stage. Cases indexed 'Second wale' and 'Both wale' present significant effect in decreasing wall deflection which reaches level of 82% of the case indexed 'General'. Measures indexed 'Top rigid' lowered deflection level to 93% of the case indexed 'General'.

(3) Wall bending moment

Fig. 18 presents varying tendency of bending moment of the wall for each stabilizing measures. It is conformed that the maximum moment arises at the depth of G.L. -6 m that is between constrain conditions of strut and embedded depth. It is estimated that only two measures, indexed 'Second wale' and 'Both wale' which exert reaction force at the depth of the maximum moment, make significant effect so that the moment is lowered to 84% of the case indexed 'General'.

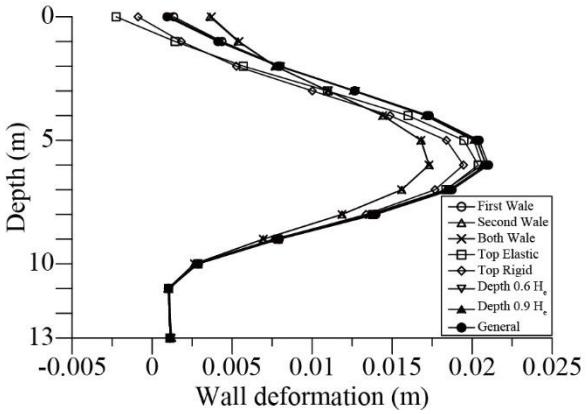

Fig. 17 Wall deflection for each case of stabilizing measures

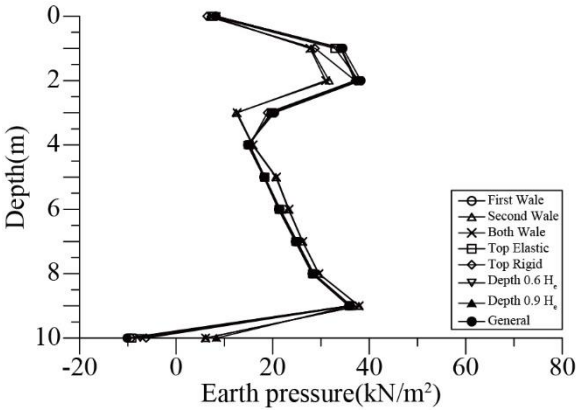

Fig. 18 Bending moment for each case of stabilizing measures

4.3 Evaluation of stabilizing measures

The comparative analysis focused on several engineering components was performed to investigate the degree of contribution of each specific measure for stabilizing the convex corner. The selected components were ground settlement, wall deflection, and bending moment. Details and results of the analysis are showed in Table 7.

Two measures indexed 'Second wale' and 'Both wale' which tie each discretized wale of two excavated sides at the intersection of the convex corner is most effective in all components of the evaluation. The number of spots that are linked by tie-material is different in those two cases, but there is little difference for stabilizing effect in quantitative terms

As tie-material for the second wale is the same condition in those two cases, the assumption that the key factor for stabilizing the convex corner is the rigid link condition in the second wale is reasonable.

It can be stated that the critical role of the tie-material at the second wale comes from the specific mode of the wall deflection. In this study, the mode of wall deflection follows deep inward mode as Ou (2006) which the strut installed at the depth of G.L. -2 m in the first excavation stage control initial deformation. Considering that, the tie-material at the

Table 7 Analysis on stabilizing measures

	First wale	Second Wale	Both Wale	Top Elastic	Top Rigid	Depth $0.6H_e$	Depth $0.9H_e$
Ground settlement	□	○	○	◎	◎	▣	▣
Wall deformation	□	○	○	◎	◎	▣	▣
Bending moment	◎	○	○	◎	○	◎	▣

○ = significant effective, ◎ = general effective, ▣ = partly effective, □ = not effective

depth of G.L. -6 m, where the maximum wall deflection arises could perform the most important role in stabilizing the convex corner.

In this study, it might be needed additional research focused on the measures for decreasing earth pressure such as reinforcing ground.

5. Conclusions

In this study, the behavioral characteristics of the convex corner for deep excavation were analyzed by the 3-dimensional numerical model. Several measures specified for the convex corner were proposed and estimated for validity. The results are summarized as follows.

- The split-shaped deformation feature of the convex corner can be simulated appropriately by introducing 'edge detached' boundary condition.
- The maximum value of deformation of plane strain condition was similar or slightly larger than for the 3D analysis, whereas the ground surface settlement behind the wall of the 3D analysis was larger than that of the plane strain condition. It was confirmed that the split-shaped behavior of the convex corner and subsequent ground surface settlement behind the wall can be conservatively simulated by 3D analysis.
- With regard to wall deflection, earth pressure, and wall bending moment, the effect of the convex corner was not distinct, whereas the maximum ground surface settlement at the convex corner was approximately 2.2 times that of middle section. The affected range of the convex corner was about the distance of the final excavation depth. The trend of stress path at the convex corner was similar to that of middle section. However, the stress path at the convex corner varied more rapidly as excavation stage progresses.
- On comparing the stabilizing measures, it was confirmed that two measures of 'linking two discretized wale at the intersection of the convex corner' and 'two points on the upper end of each wall at two excavated sides' show mechanically favorable behavior. it was found that 'linking second wale at the intersection of the convex corner' is the most effective measure for stabilizing the convex corner.
- 'Linking two discretized wale at the intersection of the convex corner' at the depth where the maximum wall deflection arise is expected to make favorable contribution not only on the deformation behavior but also on the internal force of structural member. This implies that the economic measures for stabilizing the convex corner can be introduced by estimating the deformation mode exactly.

In this paper, however we considered some typical shape of excavation corners such as convex corner with right angle. However, in urban area the shapes of corners are much more complicated due to the restriction of land use. As this research can only cover just a simple case of convex corner. It is required to investigate the effect of intersecting angles of the corners for each case.

Acknowledgments

This work is supported by the Korea Agency for Infrastructure Technology Advancement(KAIA) grant funded by the Ministry of Land, Infrastructure and Transport (Research of Advanced Technology for Construction and Operation of Underground Transportation Infrastructure, Grant 22UUTI-C157786-03).

References

Finno, R.J. and Roboski, J.F. (2005), "Three-dimensional response of a tied-back excavation through clay", *J. Geotech. Geoenviron. Eng.*, **131**(3), 273-282.

Finno, R.J., Blackburn, J.T. and Roboski, J.F. (2007), "Three-dimensional effects for supported excavations in clay", *J. Geotech. Eng.*, **133**(1), 30-36. https://doi.org/10.1061/(ASCE)1090-0241(2007)133:1(30).

Imeni, H., Ghanbari, A., Rashidi F. and Shahir, H. (2017), "Numerical study on the effect of convex corner on the behavior of deep excavations", *Elec. J. Geotech. Eng.*, **22**(10), 3965-3984.

Jeong, S.S. and Kim, Y.H. (2009), "Characteristics of collapsed retaining walls using ealsto-plastic method and finite element method", *J. Kor. Geotech. Soc.*, **25**(4), 19-29.

Lee, F.H., Yong, K.Y., Quan, K.C.N. and Chee, K.T. (1998), "Effect of corners in strutted excavations: field monitoring and case histories", *J. Geotech. Geoenviron. Eng.*, **124**(4), 339-349. https://doi.org/10.1061/(ASCE)1090-0241(1998)124:4(339).

Lee, S. and Kim, S.K. (2008), "A study on deformation analysis of the earth retaining wall", *J. Kor. Geotech. Soc.*, **24**(2), 27-36.

Mansouri, H. and Asghari-Kaljahi. E. (2019), "Two dimensional finite element modeling of Tabriz metro underground station L2-S17 in the marly layers", *Geomech. Eng.*, **19**(4), 315-327. https://doi.org/10.12989/gae.2019.19.4.315.

MIDAS (2013), GTS NX Analysis Reference.

Nian, T.K., Huang, R.Q., Wan, S.S. and Chen, G.Q. (2012),

"Three-dimensional strength-reduction finite element analysis of slopes: geometric effects", *Can. Geotech. J.*, **49**(5), 574-588. https://doi.org/10.1139/t2012-014.

Ou, C.Y., Chiou, D. C. and Wu, T. S. (1996), "Three-dimensional finite element analysis of deep excavations", *J. Geotech. Eng.*, **122**(5), 337-345. https://doi.org/10.1061/(ASCE)0733-9410(1996)122:5(337).

Ou, C.Y. (2006). Deep excavation: Theory and practice, Crc Press.

Qian, J., Tong, Y., Mu, L., Lu, Q. and Zhao, H. (2020), "A displacement controlled method for evaluating ground settlement induced by excavation in clay", *Geomech. Eng.*, **20**(4), 275-285. https://doi.org/10.12989/gae.2020.20.4.275.

Shin, J.H. (2015), Geomechanics and Engineering I, CIR, Seoul.

Szepeshazi, A., Mahler, A. and Mozcar, B. (2016), "Three dimensional finite element analysis of deep excavations'concave corners", *Per. Polytech. Civ. Eng.*, **60**(3), 371-378. https://doi.org/10.3311/PPci.8608.

Tan, Y., Wei, B., Diao, Y. and Zhou, X. (2013), "Spatial corner effects of long and narrow excavations in Shanghai soft clay", *J. Perform. Const. Fac.*, **133**(1). https://doi.org/10.1061/(ASCE)CF.1943-5509.0000475.

Wei, W.B., Cheng, Y.M. and Li, L. (2009), "Three-dimensional slope failure analysis by the strength reduction and limit equilibrium method", *Comp. Geotech.*, **36**(1-2), 70-80. https://doi.org/10.1016/j.compgeo.2008.03.003.

Xiang, Y., Goh, A.T.C., Zhang, W. and Zhang, R. (2018), "A multivariate adaptive regression splines model for estimation of maximum wall deflections induced by braced excavation in clays", *Geomech. Eng.*, **14**(4), 315-324. https://doi.org/10.12989/gae.2018.14.4.315.

Yoo, C. (2001), "Behavior of braced and anchored walls in soils overlying rock", *J. Geotech. Geoenviron. Eng.*, **127**(3), 225-233. https://doi.org/10.1061/(ASCE)1090-0241(2001)127:3(225).

Yu, Y., Damians, I.P. and Bathurst, R.J. (2015), "Influence of choice of FLAC and PLAXIS interface models on reinforced soil-structure interactions", *Comput. Geotech.*, **65**, 164-174. https://doi.org/10.1016/j.compgeo.2014.12.009.

Zhang, M., Wang, X.C., Yang, G.C. and Wang, Y. (2011), "Numerical investigation of the convex effect on the behavior of crossing excavations", *J. Zhejiang Univ.-Sci.A*, **12**(10), 747-757. https://doi.org/10.1631/jzus.A1100028.

Zhang, Y., Chen, G., Wang, B. and Li, L. (2013a), "An analytical method to evaluate the effect of a turning corner on 3D slope stability", *Comput. Geotech.*, **53**, 40-45. https://doi.org/10.1016/j.compgeo.2013.05.002.

Zhang, Y., Chen, G., Zheng, L., Li, Y. and Zhuang, X. (2013b), "Effects of geometries on three-dimensional slope stability", *Can. Geotech. J.*, **50**(3), 233-249. https://doi.org/10.1139/cgj-2012-0279.

Zhang, W., Zhang, R., Fu, Y., Goh, A.T.C. and Zhang, F. (2018), "2D and 3D numerical analysis on strut responses due to one-strut failure", *Geomech. Eng*, **15**(4), 965-972. https://doi.org/10.12989/gae.2018.15.4.965.

Zhao, W., Chen, C., Li, S. and Pang, Y. (2015), "Researches on the influence on neighboring buildings by concave and convex location effect of excavations in soft soil area", *J. Intel. Rob. Syst.*, **79**(3-4), 351-369. https://doi.org/10.1007/s10846-014-0109-7.

Zheng, G., Du, Y., Cheng, X., Diao, Y., Deng, X. and Wang, F. (2017), "Characteristics and prediction methods for tunnel deformations induced by excavations", *Geomech. Eng.*, **12**(3), 361-397. https://doi.org/10.12989/gae.2017.12.3.361.

Zdravkovic, L., Potts, D.M. and ST John, H.D. (2005), "Modeling of a 3D excavation in finite element analysis", *Geotechnique*, **55**(7), 497-513. https://doi.org/10.1680/ssc.41080.0028.